E.M.J. Stierman

# Precipitable water vapour estimation using GPS in Uganda

## Measuring and modelling the precipitable water vapour using single and dual frequency GPS receivers.


TU Delft

# Precipitable water vapour estimation in Uganda

## Measuring and modelling the precipitable water vapour using single and dual frequency GNSS receivers.

By

E.M.J. Stierman

in partial fulfilment of the requirements for the degree of

**Master of Science**
in Applied Earth Sciences

at the Delft University of Technology

| | | |
|---|---|---|
| Supervisors: | Prof. dr. Nick van de Giesen | TU Delft |
| | Dr. ir. Sandra Verhagen, | TU Delft |
| | Associate Prof. Dr. Florence D'ujanga, | Makerere University |

TU Delft

# Preface

This additional thesis is written as a part of my master program Geosciences and Remote Sensing at the Delft University of Technology. Together with Mariska Koning, I am writing a twin report. Part one determines the zenith tropospheric delay and elaborates on the precise point positioning. This part is written by Mariska Koning. The second part of the twin report is this report and is called Precipitable water vapour estimation in Uganda. I will write this part of the report. The reports should be considered together as we will refer to the two reports frequently.

Instead of following courses at the university, I choose to do an additional thesis for several reasons. First of all, it was a perfect opportunity to get more skilled in doing research and writing a scientific report. These skills will be of great use for my final master thesis. Another aspect that took my interest was the fact that this research was going to be abroad in Uganda. I have never been in a developing country for such a long time before. I want to experience how it is to live there and to set up a project. During my stay in Uganda, I expect to face many problems such as power failures and a lack of internet. Coping with this kind of problems will be a challenge but will also give me a useful experience.

This project was set up together with Prof. dr. Nick van de Giesen of the water resources management department at the Delft University of Technology. In this preface, I would like to thank him for the opportunity he gave me to go to Uganda and do a project there. Furthermore, I would like to thank Ass. Prof. Florence Mutoni D'Ujanga and Ssenyunzi Richard Cliffe for all her help in Uganda. Additionally, I would like to thank Dr. Ir. Sandra Verhagen and Dr. Ir. Hans van de Marel for supervision and helping us with questions we had about the project, equipment and software used. I would like to thank Erik Oudejans for writing the script of the single frequency receivers on the raspberry-pies. Without him, this project would not have been possible. Last but not least, I would like to thank Mariska Koning for wanting to do this research with me. She was a very good team partner.

*E.M.J. Stierman*
*Kampala, November 2016*

# Contents

# Abstract

Precipitation and especially rainfall are very important for the world's population. It has its positive and negative side like providing water and contrary causing floods. Therefore it is of utmost importance to make clear and accurate weather predictions. The revolution of GPS in the last few decades gave a new opportunity in doing atmospheric science. Many researches have been focused on atmospheric science using GPS in Europe and North America. This research gives a better insight in the precipitable water vapour in the atmosphere above Uganda. Besides weather prediction the results of this report could be used for climate studies in Africa.

Together with the research of A.M. Koning 2016 the accuracy of the to be determined zenith tropospheric delay and the precipitable water vapour in Uganda's atmosphere was determined. This study was done during the months September and October of year 2016 in the surroundings of Kampala. To obtain the precipitable water vapour, 3 measurement rounds were done. All three networks were spanned by 3 dual frequency GPS receivers densified with at least 5 single frequency GPS receivers. The ionospheric delays measured with the dual frequency receivers were interpolated to the single frequency GPS receivers so these were transformed into dual frequency receivers as well. Thereafter, the RINEX files were uploaded on the PPP NRCan application where the zenith tropospheric delay was determined. Using the constant of proportionality found by Bevis 1994 together with Saastamoinen's model to determine the zenith hydrostatic delay, the precipitable water vapour was found.

# 1. Introduction

Weather and especially rainfall, are of utmost importance for humanity. Many processes on Earth such as food production depend on fresh water and therefore rainfall. In addition, food production like crop growth and livestock production can have severe problems when amounts of precipitation are insufficient (Clark, 2012). The IPCC 5th Assessment report states that low latitude countries like Uganda will experience most climate change, with a total decrease in precipitation but an increase in extreme weather events occurring during the year (Thomas F. Stocker, 2015). In Africa, there are not many weather observations available which follow in a lack of predictions on rainfall and climate change. Therefore it is interesting to see whether or not it is possible to determine the precipitable water vapour in Uganda. Furthermore, the measurements taken can be used for further research on climate change in Uganda and even Africa.

The Trans-African Hydro-Meteorological Observatory (TAHMO) wants to set up a network of weather stations across Africa. At the moment of writing this report, 7 weather stations are in use already. These stations will likely have an affordable GPS receiver that can easily be maintained. The measurements of these devices are accessible to everyone and will help to predict rainfall and store measurements so that change in climate can be observed. The plan is to create a network which will contain 1 station per 30 $km^2$ to obtain a dense network (TAHMO, n.d.). In the last few years, a lot of improvements have been made in the world of navigation and GPS. Due to this GPS receivers become more affordable and therefore available to TAHMO as well. The aim of this research was to see if it is possible to estimate the precipitable water vapour in Uganda with an accuracy of 5-10mm using the GPS single frequency u-blox M8T antenna provided by Nick van de Giesen at the department of Water Resources at the Delft University of Technology.

Because single frequency receivers are not able to measure the ionospheric delays three dual frequency Trimble 5700 receivers provided by Hans van de Marel at the department of Geosciences and Remote Sensing at the Delft University of Technology were used in Uganda during the period of research.

Using these devices, this feasibility study found out whether or not it was possible to estimate the precipitable water vapour in the atmosphere above Uganda with the desired accuracy and distance between the receivers. Answers were found to the main question: “What accuracy can be obtained for the precipitable water vapour above Uganda when measurements are taken using dual frequency GPS receivers together with single frequency GPS/GLONASS receivers?”

This research was carried out from the 12th of September until the 4th of November of 2016 in and around Kampala, Uganda. During this period of time, the weather in and around Kampala constitutes one of the major rainfall seasons during the year (UNMA, 2016). This gave an extra dimension to this research since extreme rainfall and storms are the interest of this research and will most probably cause more precipitable water vapour in the atmosphere.

Literature studies show that the precipitable water vapour can be estimated with the desired accuracy. Though the accuracy of the precipitable water vapour depends on the accuracy of the error estimation in report 1 created by Mariska Koning, on the models used to estimate a suitable weighted mean temperature of the atmosphere and on the distance between the GPS receivers in the field. This feasibility study showed what a perfect distance was to obtain the desired accuracy for the precipitable water vapour.

This report contains a scientific background about how the precipitable water vapour is determined and how GPS errors affect the estimation of it. Results show with what accuracy the water vapour content can be obtained and at what distance the GPS receivers should be separated.

This feasibility study was carried out during September and October 2016 in Kampala and the surroundings of Kampala. Three dual frequency Trimble 5700 GPS receivers and six single frequency u-blox M8T antennas were used to get measurements of the atmosphere. Weather data was obtained from TAHMO stations located in Uganda and from the Uganda National Meteorological Authority. One of the goals was to fulfil two complete measurement sessions during the time of research.

## Locations

In Uganda, there are many different climates found reaching from wet tropical to dry desert climates. Since this research will be located in an area of 2500 $km^2$ around Kampala, a wet tropical climate is expected to be found (UNMA, 2016).

The first round was close to the capital of Uganda, Kampala, the second measurement session was carried out North-West of Kampala. Since we are working with some expensive devices, it is important to place them in areas that are secure and preferably guarded during measuring. Locations like schools, government buildings or embassies could be suitable. Furthermore, the GPS stations should have an open sky to avoid multipath errors, which will be discussed later on. To meet this requirement, locations like rooftops or open fields were appropriate.

During the first measurement session, locations to set up the dual frequency GPS stations were found in Kampala see Figure 1. Since there were no TAHMO schools inside Kampala, we interpolated weather data from other TAHMO stations to the Kampala location. The other two dual frequency receivers were located about 3-5km from the first one. The single frequency antennas were placed in between the dual frequency receivers to densify the network.

During the second measurement session, locations to set up the dual frequency GPS stations were at TAHMO schools. In this way, the GPS stations met the same conditions as the weather stations do. As reference station, the dual frequency GPS receiver at the Makerere university weree used. The two school closest to the reference station were the Ndejje Secondary school and the Mityana Secondary school. The two other GPS receivers were set up here Figure 2. Also during this measurement round, the single frequency receivers densified the network and were placed in between the dual frequency receiver network.

## Measuring devices

As stated before, three dual frequency Trimble 5700 GPS receivers with Zephyr antennas and six single frequency u-blox M8T antennas were used to get measurements of the atmosphere. The dual frequency receivers took every 15 seconds a measurement and could only receive GPS satellite signals. The single frequency antennas took every 5 seconds a measurement and can receive GLONASS and GPS satellite signals. The measurement rate of the single frequency receivers was slightly higher to see if this could increase the accuracy of the finally determined precipitable water vapour. The same reason holds for the choice of receiving two satellite constellations, GLONASS and GPS. The satellite constellations Bei Dou and Galileo were not included in this research. Bei Dou did not cover the region of Uganda. To save power, on the single frequency receiver system, we choose for the most complete constellations which were GPS and GLONASS since Galileo was not finished yet with only 14 satellites in operation in May 2016 (ESA, 2016).

Furthermore, the single frequency antennas were not supplied with a logging machine and therefore a raspberry-pi zero was used. Together with graduate student Erik Oudejans, a script was created to log the measurements taken by the M8T antennas. The measurements were stored on a micro USB card which could be read out through a UNIX computer operating system.

Weather data needed during this research were gotten from the weather stations at the TAHMO schools. The weather stations at the TAHMO schools measured the temperature and pressure every five minutes and were uploaded through their website. Because we placed one of the dual frequency GPS stations at the Makerere University in Kampala as our reference station, weather data at this location was needed as well. Unfortunately, TAHMO has no school near the university and therefore we needed to get data from the Uganda National Meteorological Authority. The UNMA had a weather station located at the Makerere University campus. Though, the accuracy of this data needs to be taken into account since the temperature and pressure were measured only twice a day and written down by hand.

## Data & Processing Software

Since the accuracy of GPS receivers increases with an increasing duration of logging the receivers should be out in the field for at least some hours (M.C. Eckl, 2001). Furthermore, it is convenient to have data of a full day so that one can see the influences of day and night on the precipitable water vapour. This means that

the receiver had to be there for at least three days, one day to setup, one day to measure and one day to dismantle the receiver.

The single frequency receivers were getting their power from power banks of 10400 mAh which meant they could run for approximately 36 hours. An improvement for further investigation could show that longer data logging of the single frequency receivers could show an improvement in the accuracy of the precipitable water vapour estimation.

Once the data was logged it was converted to RINEX format before it could be used for processing. When the datasets were obtained in RINEX format, there were several ways to determine the precipitable water vapour. One way was to get the raw data and remove all errors until the tropospheric delay is left of which the precipitable water vapour can be obtained as will be discussed in the scientific background. Another way is to use Precise Point Positioning (PPP), an online tool to determine the tropospheric delays. During this research, the last method was used. NRCAN was used for this.

Maps of the area were created in QGIS software.

## *Research Questions*

The main research question of this report are as follows.

***"What accuracy can be obtained for the precipitable water vapour above Uganda when measurements are taken using dual frequency GPS receivers and single frequency GPS/GLONASS receivers?"***

In order to answer this question, several other questions need to be answered. Those will be briefly discussed in the scientific background part of this report.

Sub-questions:
1. How is the precipitable water vapour determined using the zenith tropospheric delay?
2. Which models are available for the estimation of the zenith hydrostatic delay and which one is the most suitable for this thesis?
3. How does the distance between the GPS receivers influence the accuracy of the determined precipitable water vapour?

# 2. Scientific background

It appears that estimating the precipitable water vapour using single frequency GPS receivers in the equatorial region is a challenging task. Many errors caused in the signal path of the satellites need to be estimated. This chapter will go through all these errors briefly. Subsequently, an explanation will be given about the determination of the precipitable water content using the tropospheric delay.

## *2.1 The GPS principal*

GPS is the Global Positioning System developed by the NASA. It consists of 32 satellites orbiting the Earth. These satellites are emitting signals to Earth which are received by a GPS receiver. With the time it takes for the satellite signal to travel from the satellite to the receiver, it is possible to estimate your position anywhere on Earth at any time using a triangulation method. Since the GPS signal is travelling through the atmosphere it gets disturbed a lot by small particles. These disturbances cause an error in the signal and cause therefore a delay. In this research the delay was used to estimate the precipitable water vapour. To do this, first other errors needed to be taken into account and are discussed below.

## *2.2 Errors in GPS*

GPS would be working perfectly if there were no obstructions interfering the signal transmitted by the satellites. Though, in reality there are many errors involved in GPS. These errors can be divided in three categories, the space segment errors, the user segment errors and atmospheric errors.

### *2.2.1 Space segment errors*

Space segment errors consist of two types of errors, one is the satellite ephemeris error, the other one is the satellite clock error.

Satellite ephemeris errors occur due to inaccuracies in the satellite orbit. This orbit error can be decomposed into three components along the satellite orbit, namely radial, along-track and across-track. The error in the radial direction is small compared to the along-track and across-track errors which is fortunate since the pseudo range measurements error is in the same direction as the radial error component, the line between satellite and receiver. A Kalman filter is used to derive the ephemeris parameters (Enge & Misra, Global Positioning System, 2001).

A measurement made by a GPS receiver is actually the transit time of the signal between the satellite and the receiver, defined by the difference between the signals transmission time from the satellite and the reception time measured by the receiver (Enge & Misra, 2006). Therefore the precision of the clocks is very important and errors should be avoided. An error of 1μs can cause an offset of about 300m since the travel time is multiplied by the speed of light to get the range between satellite and receiver (Nicholas Zinas, 2016). To keep the satellite clock error as small as possible, every GPS satellite carries an atomic clock. Those atomic clocks still experience noise and clock drift errors and because of this a correction need to be made. The corrections that need to be applied are stored in the navigation file created with the measurements (Enge & Misra, 2006).

### *2.2.2 User segment errors*

There are two types of user segment errors, one is the receiver clock error, the other one is the so called multipath error.

As mentioned before, the precision of the clocks is very important. Especially for the single frequency receivers, the receiver clock error is one of the main error sources (Nicholas Zinas, 2016). The receiver clocks do not all have an atomic clock to keep them affordable. Because the satellite clock and the receiver clock are not synchronised this measurement is biased. To solve this problem, three times scales need to be taken into account: satellite clock time, receiver clock time and a common GPS Time (GPST). The satellite clock time and the receiver clock time can be related to the GPST. The biases of the satellite clock time and the receiver clock time are measured relative to the GPST and are the amounts by which the clocks are advanced to the GPST. These biases change all the time so they need constant correction (Enge & Misra, 2006).

Typically, a direct in line-of-sight measurement is received. However, the signal can also go via multiple paths, having reflected on surrounding objects or via the ground to the receiver. A multipath is longer than the direct line-of-sight to the satellite and therefore introduced a delay in both the measurements (Enge & Misra, Global Positioning System, 2001). The multipath signals can be characterised by their amplitude, the signal is usually weaker than the direct signal, the delay of the signal, its phase and phase rate of the reflected signal with respect to the direct signal. When multiple waves coming in simultaneously, interference will occur and the multipath signals will thus distort the direct signal (K. Yedukondalu, 2011).

### *2.2.3 Atmospheric errors*

Since the GPS signal is travel through the atmosphere it is affected by the ionosphere and the troposphere causing 2 delays. These delays need to be removed and corrected for in order to find eventually the precipitable water vapour.

#### *2.2.3.1 Ionospheric delays*

The ionospheric delay can only be measured using the dual frequency GPS receiver measurements. The ionosphere is a region ranging from 50 km to about 1000 km above the Earth's surface in which free electrons and ions are situated. Ionisation is caused by Solar radiation which causes refraction of the transmitted satellite signals. As the physical characteristics depend greatly on the Sun, day and night differences are large. During the day, molecules are broken up in ions and electrons and thus the electron density increases. However, when the Sun has set, the ions and electrons recombine again, reducing the electron density. The speed of propagation of radio signal depends on the number of electrons that it encounters when propagating to the medium. Therefore a parameter called 'total electron content' (TEC) is taken into account. TEC means the number of electrons which are encountered in a column of 1 $m^2$ cross section extending from the satellite to receiver. One way to eliminate the ionospheric delay is to use an ionospheric-free combination. The estimate of the ionospheric group delay at L1 frequency and L2 frequency using the code measurements are:

$$I_{L1} = \frac{f_{L2}^2}{f_{L1}^2 - f_{L2}^2}(\rho_{L2} - \rho_{L1}) \quad (1)$$

$$I_{L2} = \frac{f_{L1}^2}{f_{L1}^2 - f_{L2}^2}(\rho_{L2} - \rho_{L1}) \quad (2)$$

In which $I_{L1}$ and $I_{L2}$ stand for the ionospheric delays on the L1 and L2 frequency bands respectively, $f_{L1}$ and $f_{L2}$ stand for the frequencies of the L1 and L2 frequency bands, the $\rho_{L1}$ and $\rho_{L2}$ stand for the code measurements on band L1 and L2 respectively (Enge & Misra, Global Positioning System, 2001).

Since the TEC is very variable in equatorial regions and thus the ionospheric delay as well, it is of utmost importance to determine this error very accurately (Enge & Misra, 2006). A better insight into the ionospheric variation in the region of Uganda is described by A.M.Koning (Koning, 2016). The most suitable way in determining the ionospheric delay component is described here as well. When the ionospheric delay is determined it can be subtracted from the pseudorange measurement so the ionospheric-free pseudorange is obtained.

#### *2.2.3.2 Tropospheric delays*

When the ionospheric delay is removed, the remaining parts are electrically neutral and non-dispersive to the frequencies used in GNSS measurements. The tropospheric delay consists of two components: a hydrostatic component, depending mostly on dry gasses, and a wet component that depends on the moisture content. The former component accounts for approximately 90% of the delay, but the variation in the delay is much larger in the wet delay, as this component varies more both spatially and temporally. The dry component can be modelled to the millimeter level accuracy (Gabor, 1997). The dry and wet component together, are zenith tropospheric delay.

From the total delay of the signal, first Zenith Tropospheric Delay (ZTD) is estimated. This can be seen as the total delay caused by the troposphere in zenith direction. The ZTD in this research is found using PPP (Precise Point Positioning) using the online NRCAN web-application. This website uses dual frequency GPS receiver observations to estimate the ZTD and its standard deviation. For the single frequency receiver observations an extra created observation is added to the observations. This extra observation will be created using an inverse distance interpolation of the dual frequency receiver observations. In this way, an L2 observation is created at the locations of the single frequency receivers (Koning, 2016).

The dry component of the zenith tropospheric delay can also be called the Zenith Hydrostatic Delay (ZHD) and is estimated by a model based on accurate pressure measurements at the GNSS station (Gabor, 1997). In this research, these pressure measurements will be obtained from the TAHMO weather stations.

The wet component of the zenith tropospheric delay can be called the Zenith Wet Delay (ZWD). The ZWD can be calculated by subtraction of the ZHD from the ZTD, the relation between those is as follows (K. Yedukondalu, 2011).

$$ZTD = ZHD + ZWD \tag{3}$$

## 2.3 Determining the Zenith Hydrostatic Delay (ZHD)

As said before, the ZHD can be determined using models with accurate pressure measurements. These pressure measurements are obtained at the TAHMO weather stations located at the schools where the dual frequency GPS receivers will be placed. In this manner, an environment will be created that is similar for the weather station and the GPS receiver to reduce the differences between those.

There are many models which can determine the ZHD (Shrestha, 2003). The three which are mostly used will be discussed below.

### 2.3.1 Saastamoinen model

Saastamoinen assumed hydrostatic equilibrium so the hydrostatic delay could be determined by a function using a measure of surface pressure (Shrestha, 2003). This model is dependent on the choice of refractivity constants and on the modeling of the height and latitude dependence of the acceleration of gravity (V.B.Mendes & R.B.Langley, 1999). The refractivity constants of Essen and Froome (1951) were used to get the following expression for the zenith hydrostatic delay.

$$ZHD = \frac{0.002277 P_s}{(1 - 0.0026 cos 2\phi - 0.00000028 H_s)} \tag{4}$$

In which $P_s$ is the surface pressure, $H_s$ is the receiver height and $\phi$ is the latitude of the receiver.

### 2.3.2 Baby et al. model

Another model dependent on the choice of refractivity constants and on the modeling of the height and latitude dependence of the acceleration of gravity is the baby et al. model (V.B.Mendes & R.B.Langley, 1999). The K1 refractivity constant is developed by Bean and Dutton (1966) in this model. Baby et al. created a theoretical which is as follows (Shrestha, 2003):

$$ZHD = \frac{0.022277 P_s}{g_s}\left[1 + \frac{2}{r_s \sigma(\mu + 1)}\right] \tag{5}$$

In which $g_s$ is the gravity at the surface, $r_s$ is the mean geocentric radius of the station in meters. The parameters, $\sigma$ and $\mu$ are given by the following expression respectively.

$$\sigma = \frac{\alpha}{T_s} \qquad \mu = \frac{g_s}{R_d \alpha}\left[1 - \frac{2}{r_s \sigma}\right] \tag{6}$$

In which $\alpha$ is the lapse rate, $T_s$ is the surface temperature and $R_d$ is the specific gas constant for dry air.

### *2.3.3 Hopfield model*

The Hopfield model uses a quartic model for the determination of the ZHD. And states as follows (V.B.Mendes & R.B.Langley, 1999):

$$ZHD = 10^{-6} N_{ds} \frac{H_d^e - H_s}{5} \tag{7}$$

In which $N_{ds}$ is the dry refractivity factor at the surface, $H_d^e$ is the equivalent height which can be expressed as 40136+148.72(T-273.16) (Shrestha, 2003), $H_s$ is the height of the receiver.

### *2.3.4 Model in this research*

Since there are many models which are determining the ZHD and this research is bound to a period of 2 months only, a choice is made to use the Saastamoinen model to determine the ZHD. This choice is based on the papers of Mendes et al. 1999 and De Haan 2016 (V.B.Mendes & R.B.Langley, 1999) (Haan, 2008). In this paper a research on the accuracy of those three models is described. Mendes compared their findings with radiosonde data to which there is no availability in this research. Based on their conclusions we can find the ZHD within an accuracy of sub-millimeter level (V.B.Mendes & R.B.Langley, 1999).

## *2.4 Determining the precipitable water vapour*

Once the zenith hydrostatic delay and the zenith tropospheric delays are estimated, the zenith wet delay can be calculated by subtracting the ZHD from the ZTD. After this, the precipitable water vapour can be estimated. Precipitable water vapour is known as the vertically integrated water vapour overlying a receiver, in terms of an equivalent column of liquid water (M. Bevis, 1994). When the ZWD is known, the precipitable water vapour can be calculated using a dimensionless constant of proportionality (M. Bevis, 1994) (Yuan, 2014).

$$PWV = C * ZWD \tag{8}$$

In which C is the dimensionless constant of proportionality and ZWD is the zenith wet delay. According to *Bevis et al. 1994*, the constant of proportionality:

$$C = \frac{10^6}{\rho_w R \left(\frac{K_3}{T_m} + K_2 - \frac{M_w}{M_d} K_1\right)} \tag{9}$$

Where $\rho_w$ stands for the density of liquid water, R for the specific gas constant of water vapour, $T_m$ is the weighted mean temperature of the troposphere. $M_w$ and $M_d$ are the molar masses of water vapour and dry air respectively. The constants, $K_1$, $K_2$, and $K_3$ are the constants for refractivity (M. Bevis, 1994). These constants are determined by many authors, for example Smith and Weintraub; Thayer; and Hasawaga and Strokesbury (M. Bevis, 1994). In 2002 Rüeger et al. stated that the 'best average coefficients are as follows. K1=77.6890 K/hPa, K2=71.2952 K/hPa and K3=375463 $K^2$/hPa (J.M.Rüeger, 2002). In this research these values for the constants will be used as well. For $M_w$ and $M_d$ values of 0.018016 kg/mol and 0.028964 kg/mol will be used respectively (Yuan, 2014). As a gas constant the value of 8.314462 J/K/mol will be used. The density of liquid water is 999.9720 kg/$m^3$. When all those values are substituted into the formula a constant of proportionality is obtained which is dependent on the weighted mean temperature only. The weighted mean temperature can be obtained numerically, but due to time limitations the Bevis model for this constant will be used.

$$T_m \approx 70.2 + 0.72 T_0 \tag{10}$$

Here, $T_0$ is the surface temperature at the location of the receiver and is given in Kelvin. Once all those values are known, an estimation for the precipitable water vapour in the atmosphere above Uganda can be made.

## 2.5 Interpolation technique

To derive values on locations where no measurements are taken an inverse distance interpolation will be used in this research. In this section, this technique will be briefly discussed. Inverse distance interpolation gives a weight to each of the existing data points. The weights of the points closer to the unknown point get a larger weight. Instead of giving all the weight to the points close by, a power 2 is used to decrease the weight slightly (Wackernagel, 2003). The equation used for inverse distance interpolation is as follows.

$$u(x) = \sum_{i=1}^{N} w_i(x) u_i \tag{11}$$

$$w_i = \frac{1}{d_i} \tag{12}$$

In which w represents the weight for each of the values to be interpolated, $u_i$ is the $i^{th}$ value to be interpolated, d is the distance from each point to the unknown value position. Using this formula all the values are taken into account and the values which are closest to the unknown point has the height weight, the value furthest away gets the smallest weight.

Since there is no weather data available at the Makerere university, weather data from the TAHMO weather stations around Makerere university are interpolated in this way. This counts as well for the single frequency receivers which are placed in between the dual frequency stations. The interpolated weather data is later on used to determine the ZHD at each location. Furthermore the ionospheric delays measured at the dual frequency stations need to be interpolated to the locations of the single frequency receivers. The single frequency observations are then converted into dual frequency measurements.

## 2.6 Error propagation

To know the accuracy of the determined PWV at the receiver locations error propagation is executed on the standard deviation of the ZTD obtained from the PPP process. The PPP application also presents the determined standard deviations of the ZTD. These values will be used to calculate the standard deviation of the PWV. According to Yuan 2014 the values for ρ, R, $M_w$, $M_d$, $K_1$, $K_2$, $K_3$ can be assumed to be constant. Also the values for the ZTD, ZHD and $T_m$ are assumed to be independent and therefore error propagation can be used to determine the standard deviation of the PWV (Yuan, 2014). When error propagation is applied, the standard deviation for the PWV is as follows.

$$\sigma_{PWV} = \sqrt{\left(\frac{10^6}{\rho R\left(K_2 - \frac{K_1 M_w}{M_d} + \frac{K_3}{T_m}\right)}\right)^2 (\sigma_{ZTD}^2 + \sigma_{ZHD}^2) + \left(\frac{10^6 K_3}{\rho R\left(K_2 T_m - \frac{K_1 M_w}{M_d} T_m + K_3\right)^2}\right)^2 ZWD^2 \sigma_{T_m}^2} \tag{13}$$

$$\sigma_{ZHD} = \sqrt{\left(\frac{0.002272}{1 - 0.0026cos2\phi - 0.00000028H_s}\right)^2 \sigma_P^2 - \left(\frac{0.002272}{(1 - 0.0026cos2\phi - 0.00000028H_s)^2}\right)^2 \sigma_H^2} \tag{14}$$

In those equations σ represents the standard deviation of each variable.

# 3. Network Set-up

This research was taking place in Uganda. Since Uganda has many different climates, the research area focused on will be reaching up to 60km West and 30km North of Kampala. It was assumed that the climate in this area is similar everywhere so this would not affect the research drastically.

The time span was two months and measurements were taken during the months of September and October. These months were supposed to be rainy months with great amounts of precipitation (UNMA, 2016), in the end it turned out it was a very dry season. This could be possibly the result of climate change as the IPCC stated (Thomas F. Stocker, 2015). But since there is no extensive monitoring of climate in Africa yet, this expectation is not proven yet. This is one of the main reasons for this research, monitoring the climate in Africa.

During those two months two measurement rounds were planned. The first one had its focus on the area of Kampala. The second one had its focus on the expanded region as stated before. In this chapter those two measurement rounds will be briefly described.

## *3.1 Ideal network*

To obtain a higher spatial resolution of the estimated ZTD it is of great importance to have enough GNSS measurements (Deng, 2009). Since dual frequency receivers are expensive and sparse in Uganda, single frequency GPS receivers will be used to densify the desired network (Deng, 2009).

Several researches have been done on the network design of GPS stations to measure the PWV in the atmosphere (J. Braun, 1999; Yoshinori Shoji, 2014; D. E. Wolfe, 1999; C. Rocken, 2000). Yoshinori Shoji 2014, showed that a GNSS network with a spacing of 17km between the receivers could not always measure severe storms, but for monitoring heavy rainfall in Japan it was sufficient enough (Yoshinori Shoji, 2014). The GNSS station network in Japan is one of the densest networks in the world (Yoshinori Shoji, 2014; C. Rocken, 2000).

According to Rocken 2000, a GPS network consisting of single frequency GPS receiver and dual frequency GPS receivers can measure the PWV accurately when the dual frequency receivers have a spacing of approximately 35-150km (C. Rocken, 2000). The spacing of the dual frequency receivers is of great importance to determine the ionospheric delay. In this research, the ionospheric delay found at the dual frequency locations will be interpolated to the single frequency receivers. Rocken 2000 also showed that a network of dual frequency GPS receivers spaced 30-40km could be interpolated and accurately determine the ionospheric delay at the single frequency locations. Though, it has to be taken into consideration that the research of Rocken was carried out in Colorado, a mid-latitude region and this research is carried out in Uganda which is located in the equatorial region.

Braun 1999 showed that using 20 single frequency GPS receivers spanning a network of 10-20km can determine the PWV accurately in Colorado (J. Braun, 1999). For the ionosphere a model was used.

The GPS PWV estimation closely depends on the accuracy and the precision of the ZTD estimation. GPS stations having baselines smaller than 10km show a standard deviation in the ZTD of about 6mm (E. R. Westwater, 1998). An error of this magnitude in the ZTD causes 1mm error in the PWV estimation (D. E. Wolfe, 1999).

This research will be carried out in a region around the equator. In the equatorial region the PWV can be very inhomogeneous and is therefore difficult to obtain (S. Amir, 2011). Another point of issue is that there are not many measurement devices available in those regions. Because of this, a network needs to be designed suitable for this region. Since the ionosphere in this region is inhomogeneous and changes with the time during the day a lot the separation of the dual frequency receivers Rocken 2000 mentioned could be sparse. Therefore we choose to distribute the dual frequency GPS receivers with a separation on the lower side of this margin, so approximately 35-100km apart. The single frequency receivers should be spread out as evenly

as possible between the dual frequency receivers (M. Bender, 2009). In this research, the desire was to mimic the ideal network as much as possible during the measurement rounds. First a small network was created to test the equipment, thereafter a larger network was created.

## 3.2 Measuring round one

Measuring round one took place within the capital of Uganda, Kampala. This location was chosen in order to reach GPS receivers facing problems quickly. The main idea about this measuring round was to check if all equipment was working as expected and to experience the workflow in Uganda. Besides this the accuracy of the dual and single frequency GPS receiver was tested when those were located closely together.

In this measuring round all of the three dual frequency GPS receivers were used. It was hard to find those receivers a secure but open place in a crowded city like Kampala. Several schools were inquired but were always unsuccessful in the end. One of the receivers was placed on the roof of the physics department building at the campus of the Makerere University on the 19th of September (dual frequency receiver 1). This station was used as a reference station during the whole project. Another GPS receiver was placed at the roof top of someone's house (dual frequency receiver 2), about 4km East of the chosen reference station location. This station was placed at this location on the 20th of September. The third and last dual frequency receiver was placed on top of the TAHMO guesthouse building on the 21st of September (dual frequency receiver 3). The TAHMO guesthouse is located about 7km North-East of the reference station. Using QGIS a map was created of the receiver locations within Kampala, Figure 1. Dual frequency receiver number 2 was picked up on the 30th of September and dual frequency receiver number 3 was picked up on the 29th of September. All receivers seemed to have worked perfectly and the data looked promising.

Since the dual frequency receivers need some time to get the desired accuracy and precision in location estimations it was decided to start placing the single frequency receivers on the 27th of September. A limitation for the single frequency GPS receivers was that these could only run for 36 hours due to the energy limit of the power banks suppling those receivers. In this measuring round, five single frequency GPS receivers were used. These receivers were placed in between the dual frequency receivers including one of them exactly at the reference station. Another receiver was placed on top of the Arcadia Hotel, about 1.5km East of the reference station. Two single frequency receivers were placed North-East of the reference station, one of them on top of a toilet building 4km away, the other one on the guardhouse of the IITA 4.5km away. The last of the five single frequency receiver was placed in the garden of the house we stay, 0.5km West of the reference station. Figure 1 gives an overview map of the locations of the dual and single frequency receiver locations.

All the single frequency receivers were picked up on the 28th of September. Unfortunately, the receiver placed on top of the toilet building was drowned by rainfall and therefore no data was logged. The receiver located at the reference station did not log data as well for a yet unknown reason.

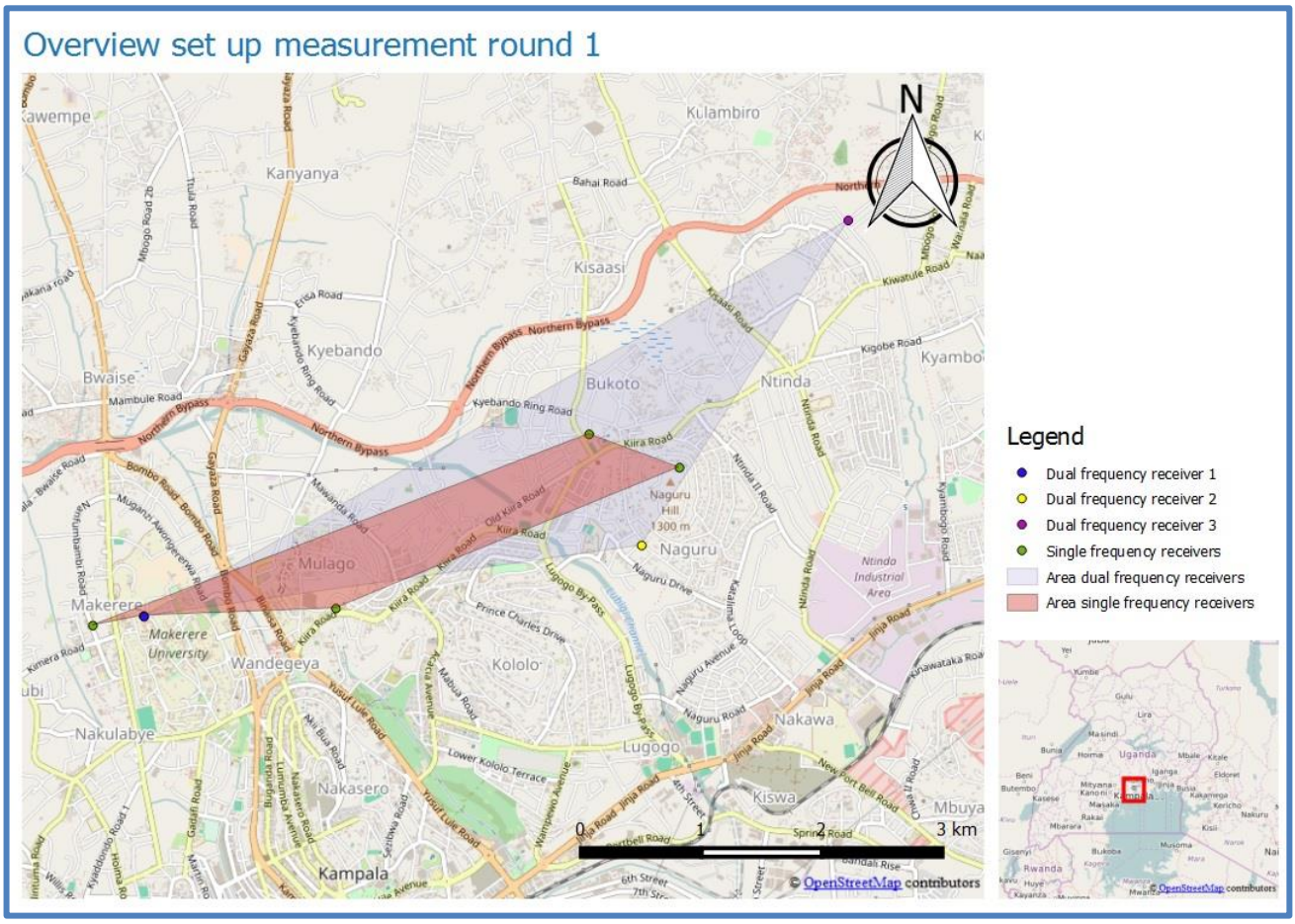


**Figure 1: Overview of set up measurement round 1.**

## *3.3 Measuring round two*

After having finished the first measuring round, a second measuring round was executed. The area of the second measuring round was approximately 900km$^2$. The main idea of this measuring round was to create network larger than the first network

Dual frequency receiver number 1 was still located at the Makerere University in Kampala as a reference station. The second dual frequency receiver was placed at the Mityana Secondary School, about 60km West of Kampala on the 5$^{th}$ of October. It was placed on a water tank so it had an open view to the sky. The third dual frequency receiver was placed at the Ndejje Secondary School, about 30km North of Kampala on the 3$^{rd}$ of October. This receiver was placed on top of a flat rooftop. Both receiver were chosen to be placed at those schools because these schools had a TAHMO weather station. In this way, the conditions between the dual frequency receiver measurements and the weather measurements were kept the same. An overview of the dual frequency receiver locations can be found in Figure 2. Dual frequency receiver 3 was picked up on the 12$^{th}$ of October. Dual frequency receiver 2 was picked up on the 14$^{th}$ of October. Unfortunately, dual frequency receiver number 2 stopped working after 3 days of recording without our notice before.

The single frequency receivers were placed in between the dual frequency receivers on the 10$^{th}$ of October. During this measurement round five single frequency receivers were used. We tried to distribute those as evenly as possible. Figure 2 shows where the single frequency receivers were placed. One of the receivers was placed on a water tank at the Makerere University. Another single frequency receiver was placed North of the reference station in Kampala at around 20km distance on a water tank at the Makerere high school. Two of the receivers were placed West of Kampala at a distance of 15km and 35km on the roof of Richard Cliffe's house and on the rooftop of the Modern primary school in Jezza respectively. The last single frequency receiver was placed on a water tank at the Wakiso district headquarters. In this way, all the single frequency receivers were located in a secure but with an open face to the sky. When the single frequency receivers were picked up, on the 12$^{th}$ and 13$^{th}$ of October they all seemed to have worked well except of the one at the Makerere University.

Many problems were faced during this measurement round, dual frequency receiver 2 stopped working and the single frequency receiver at the Makerere University as well. In this research, interpolation would have been used for the ionospheric delay measured by the dual frequency receivers, to obtain ionospheric delays at the single frequency receivers. Since dual frequency receiver 2 stopped working on the 8th of October and the single frequency receivers were set up on the 10th of October there was no data available of these devices at the same moment. Therefore the ionospheric delay at the single frequency receiver locations cannot be determined and it was decided to execute another measurement round.

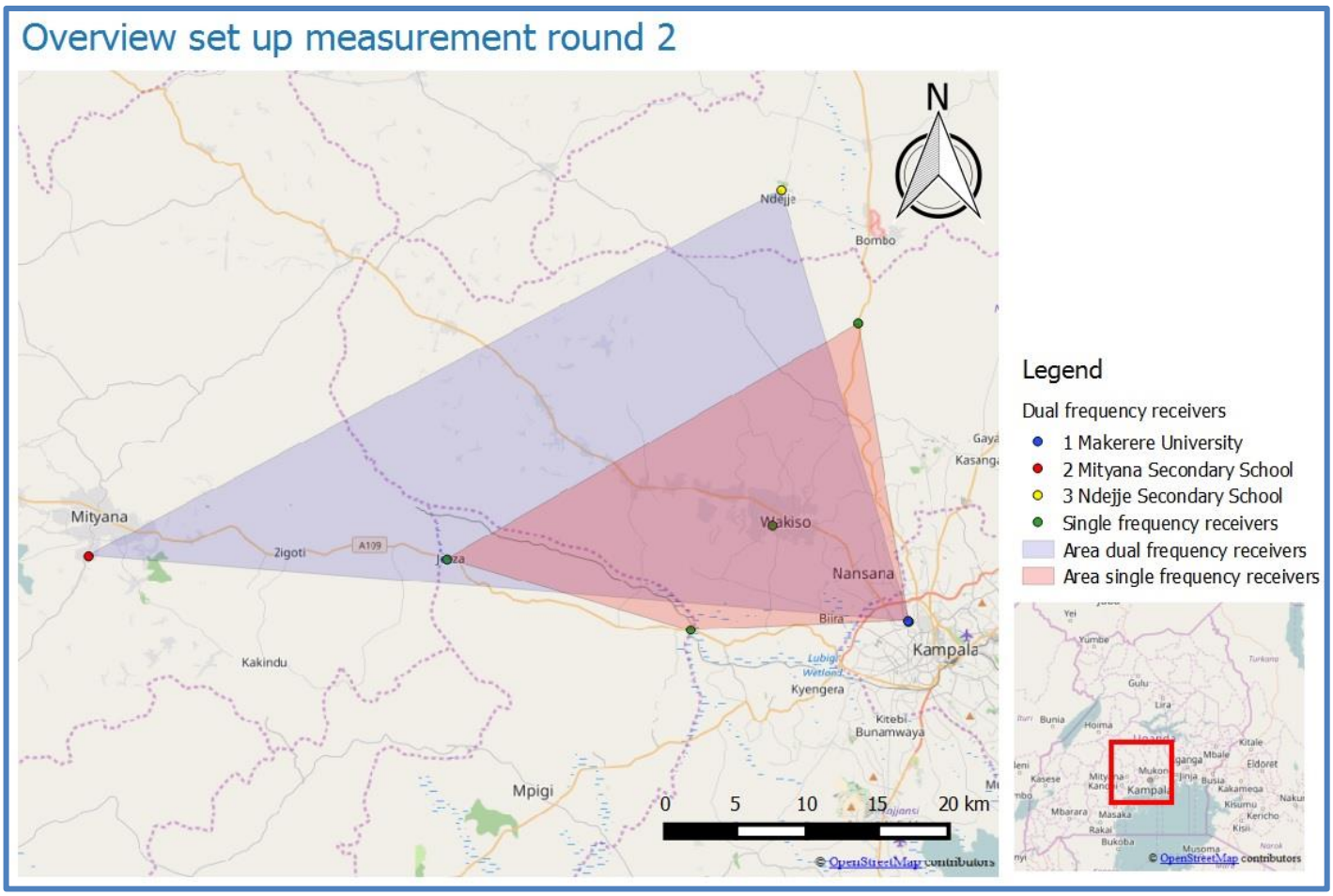


Figure 2: Overview of set up measurement round 2.

## 3.4 Measuring round three

During the second measurement round, desired measurements were not obtained due to the logging failure of the second dual frequency receiver. Therefore the third measurement round was executed. The area of the third measurement round had an area of approximately 1500km$^2$ and was located North-East of Kampala.

The first dual frequency receiver was still located at the Makerere University as a reference station. Another receiver was placed at the Ndejje Secondary School again on the rooftop on the 17th of October. Since the dual frequency receiver failed to work at the Mityana Secondary School in the previous measurement round, it was decided to place the third receiver at another location. Therefore the third dual frequency GPS receiver was placed at the Wanyange Girls Secondary School, located approximately 100km East of Kampala. The receiver was placed on top of the guards house to have an open view to the sky and was also secured. This receiver was placed there on the 18th of October. Also the Wanyange Girls Secondary School has a TAHMO weather station so the conditions for this GPS and the weather measurements are the similar. An overview of the locations of the dual frequency GPS receivers can be found in Figure 3.

The single frequency receivers were placed in between the dual frequency receiver as evenly distributed as possible on the 25th of October. One of the receivers was placed at the Makerere University again together

with the reference dual frequency GPS receiver. Two single frequency GPS receivers were placed in between Ndejje and Kampala. One of these was placed on a water tank at the World Ahead Senior Secondary School, approximately 10km North of Kampala in Matugga, the other one was placed at the Makerere high school on top of a water tank about 20km North of Kampala in Migadde. Two other single frequency receivers were placed between Kampala and the Wanyange Girls Secondary School. One was placed on top of the entrance gate of the Homeland College in Lugazi, about 50km East of Kampala, the other one was placed on the rooftop of the Colline Hotel in Mukono approximately 20 km East of Kampala. The last single frequency receiver was placed on top of a water tank at the African Village Hotel near Kayunga, which is approximately 30km North-East of Kampala. All receivers are placed above buildings so that multipath errors could be limited. An overview of the setup locations can be found in Figure 3.

All the dual and single frequency receivers were picked up on the 27th of October. They all seemed to have worked fine and had some overlapping time and thus data. Therefore this data will be worked with during the processing and producing a PWV map.

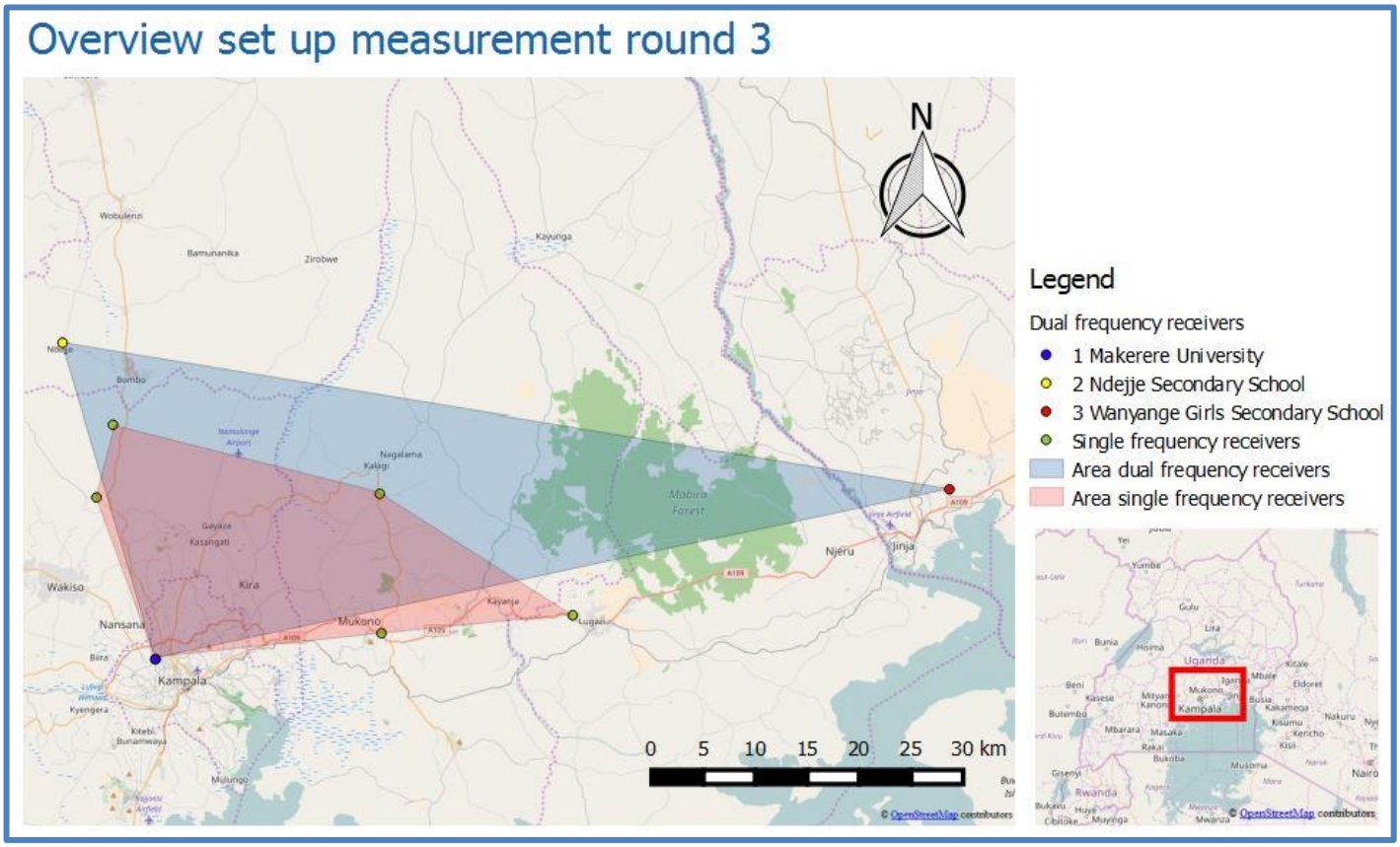


**Figure 3: Overview of set up measurement round 3**

# 4. Processing

In this chapter the processing steps undertaken to derive the precipitable water vapour will be discussed. Per data set we will go through the whole process. Since all the data sets are running in different time settings it was important to get all data set in the right time zone. A flowchart was created of the total process and is shown in Figure 4.

## 4.1 Weather data

The weather data provided by the TAHMO weather stations logged measurements every 5 or 10 minutes. Therefore the weather data was filtered with time intervals of 10 minutes. The time flag of the weather data was in the Ugandan time zone which is UTC+03:00. Every time the weather data was used a subtraction of 3 hours needed to be applied to get the weather data in UTC.

Another issue that occurred during this research was the fact that there was no weather data available at the reference dual frequency GPS station at the Makerere University. The Ugandan National Meteorological Authority did have a weather station at the university campus but did not want to provide the data. In order to derive the ZHD at the reference station pressure at location must be known. To solve this issue, the interpolation method discussed in chapter 3.4 was used to obtain the pressure at the reference station. In the interpolation method the TAHMO weather measurements at the Ndejje Secondary School, Mityana Secondary School, Wanyange Girls Secondary School and Entebbe WME were used. For the temperature used in the constant of proportionality to derive the PWV, the temperatures from the 4 named TAHMO weather stations were interpolated to the reference station as well.

Furthermore, the right time slot overlapping the single frequency receivers data was selected

## 4.2 Dual frequency data

The dual frequency receivers logged data every 15 seconds. To obtain the ZTD from the dual frequency data the data files were uploaded on the NRCan PPP (Natural Resources Canada) processing application. This online application provides the ZTD per time step with its standard deviation. This tool uses Precise Point Positioning to determine the desired parameters like positions and ZTD. Precise Point Positioning is discussed in more detail in the report of A.M. Koning 2016 (Koning, 2016). The time flag used in the GPS measurements is in UTC time.

## 4.3 Single frequency data

The single frequency receivers logged data every 5 seconds. Using the Teqc software program the measurements every 15 seconds were selected so they overlap with the dual frequency measurements.

For the ionospheric correction a dual frequency measurement is needed. Since the single frequency receivers have only measurements taken on one frequency namely the L1 band other measurements needed to be created on another frequency. In this way, the single frequency measurements could be converted into dual frequency measurements. The single frequency receivers have only C1 and L1 observation, respectively the pseudorange code measurements and the carrier phase measurements. Using the principal of Deng et al. 2009, a C2 and L2 measurement on the second frequency was generated for the single frequency receivers (Deng, 2009). For the C2 observation the following equation was used.

$$C_2 = C_1 - I_{c1} + I_{c2} \tag{15}$$

In which C1 is the pseudorange observation of the single frequency receiver, $I_{c1}$ and $I_{c2}$ are the ionospheric delays on the C1 and the C2 measurements respectively. So first an ionospheric free C1 observation was created by subtracting the ionospheric delay of the first frequency from the C1 observation in order to add the ionospheric delay for the C2 observation. The ionospheric delays were found using the observations of the dual frequency receiver and interpolating those ionospheric delays to the single frequency receiver locations. The ionospheric delays on the C1 and C2 could be found using the following equations.

$$I_{c1} = \frac{f_2^2}{f_1^2 - f_2^2}\,(C_2 - C_1) \qquad I_{c2} = \frac{f_1^2}{f_1^2 - f_2^2}(C_2 - C_1) \tag{16}$$

In which $f_1$ and $f_2$ are the first and second frequency respectively, the $C_1$ and $C_2$ are the pseudorange measurements of the dual frequency receivers.

Also a carrier phase measurements for the second frequency had to be created at the single frequency receiver locations. In order to do so, the following equation was used.

$$L_2 = L_1 - L_4 \tag{17}$$

In this equation $L_4$ is the ionospheric observation and $L_1$ is the carrier phase observation on the first frequency of the single frequency receiver. According to Deng et al. 2009 the ionospheric observation could be calculated using an epoch differenced method. In which the epoch differenced ionospheric delays are calculated in the following way.

$$D(i-1,i) = \frac{f_2^2}{f_1^2 - f_2^2}\left((\lambda_1 L_1^{i-1} - \lambda_2 L_2^{i-1}\right) - (\lambda_1 L_1^i - \lambda_2 L_2^i)) \tag{18}$$

Here the $\lambda_1$ and $\lambda_2$ are the wavelengths of the first and second frequency respectively, the $L_1^{i-1}$ and the $L_2^{i-1}$ are the carrier phase observations during the i-1$^{th}$ epoch on the first and second frequency of the dual frequency receivers. The $L_1^i$ and the $L_2^i$ are the carrier phase observations during the i$^{th}$ epoch on the first and second frequency of the dual frequency receivers. From the epoch differenced ionospheric delays, the ionospheric observation, $L_4$, could be calculated by taking the sum of all the epoch differenced ionospheric delays.

$$L_4^i = \sum_0^{i-1} \frac{f_1^2 - f_2^2}{f_2^2} D(i-1,i) \tag{19}$$

In this equation $L_4^i$ is the ionospheric observation for epoch I, D(i-1,i) is the epoch differenced ionospheric delay between epoch i-1 and i. Using this generated L4 an L2 observation for the single frequency receivers was created.

When the single frequency receiver observations had an C1, C2 and an L1 and L2 observation, they were uploaded in the NRCan PPP application as dual frequency receivers and thereto a ZTD value was derived for the single frequency receivers as well.

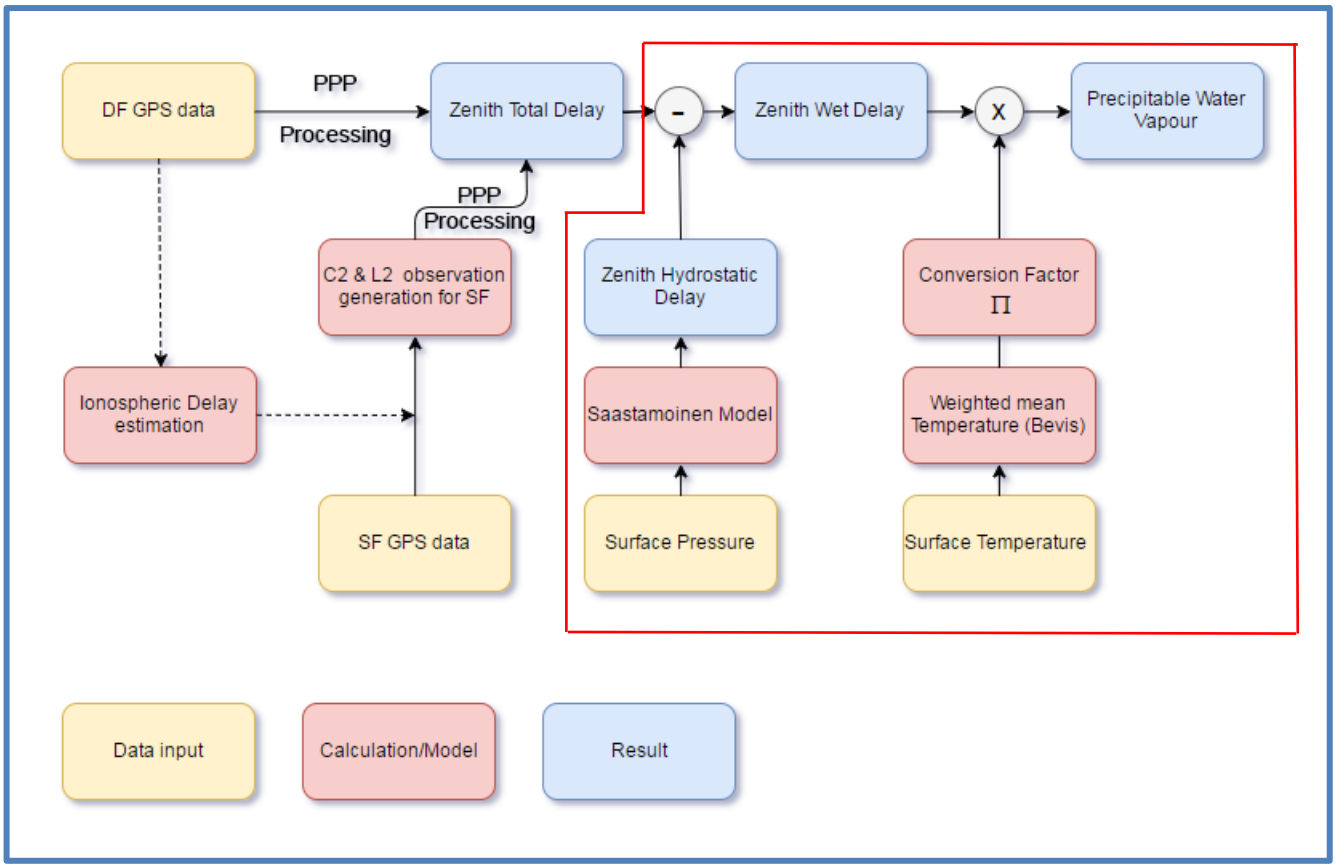


Figure 4: Flowchart of the total process

# 5. Results & Discussion

In this chapter the results will be presented. Since there was a failure of one of the dual frequency GPS receivers during the second measurement round, the data of that measurement round was left out. The results of measurement round 1 and 3 will be presented.

Since the resulting PWV estimations are very dependent on the results of the ZTD estimation from the PPP processing, the standard deviations of the ZTD and the height estimation will be used to calculate the standard deviation of the estimated PWV using error propagation.

## *5.1 Measurement round 1*

During measurement round 1 three dual frequency receivers were placed in the surroundings of Kampala together with 5 single frequency receivers in between the dual frequency receivers. Table 1 gives an overview of the performance of all those receivers.

Table 1: Overview of devices and their performance during measurement round 1.

| Receiver | Location | Logging time (UTC+3) | Remarks |
|---|---|---|---|
| Dual 1 | Makerere University | 26 Sept 10:26-<br>29 Sept 03:00 | - |
| Dual 2 | House | 22 Sept 03:00-<br>29 Sept 03:00 | Not perfectly levelled when picked up |
| Dual 3 | TAHMO office | 22 Sept 03:00-<br>29 Sept 03:00 | - |
| Single 1 | Makerere University | 27 Sept 19:45-<br>28 Sept 11:44 | Multipath error, many buildings in the surrounding |
| Single 2 | Arcadia Hotel | 27 Sept 17:45- | - |

| | | | |
|---|---|---|---|
| | | 28 Sept 16:48 | |
| Single 3 | Toilet Building | Failed | Flooded by the rain after 5 minutes |
| Single 4 | IITA | 27 Sept 15:45-<br>28 Sept 16:07 | - |
| Single 5 | Home | 27 Sept 20:15-<br>28 Sept 11:38 | Multipath error, many buildings in the surrounding |

### *5.1.1 PWV estimations with their standard deviations*

The precipitable water vapour estimations for the dual and single frequency receivers are calculated using equation 8. The PWV estimation for the dual frequency receivers is shown in figure 5. The standard deviations calculated using equation 13. for the dual frequency receivers are shown in figure 6. For the single frequency receivers the PWV estimation is plotted with a positive and negative error bar based on the calculated standard deviation. These results are shown in figures 7 to 10.

*Dual frequency receivers*

In Figure 5 it is shown that the three dual frequency receivers had an estimated precipitable water vapour of about 2 cm. There are small variations in the estimations. The estimated PWV of the House has a notable dip around 18.45. The standard deviations of the PWV estimations stay small for the dual frequency receivers as shown in Figure 6. The standard deviations stay all around 0.35 mm which means there is an error of about 1.75%.

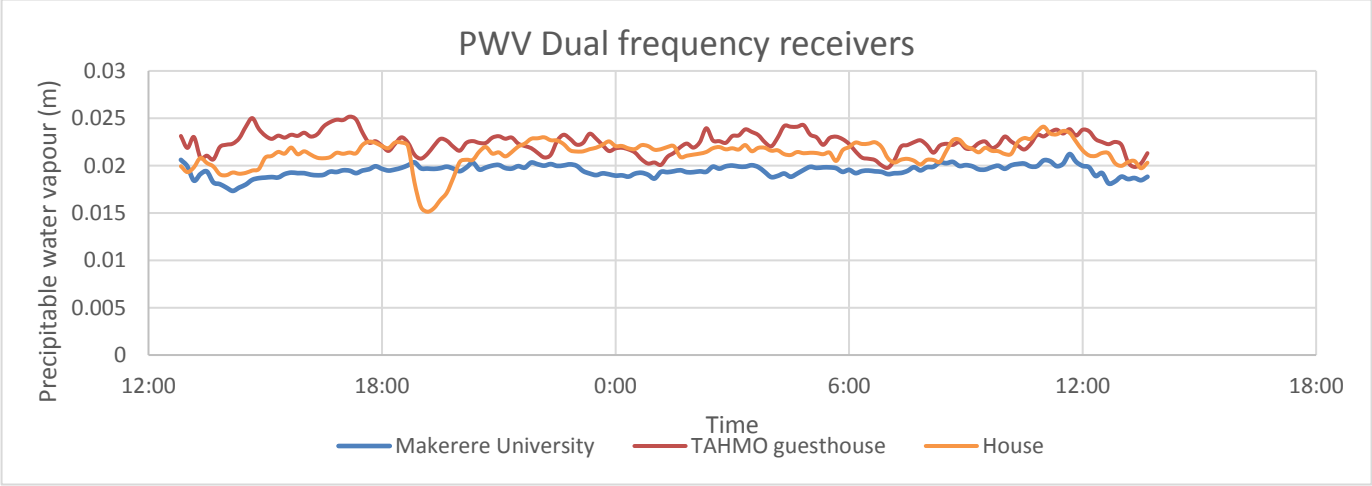


**Figure 5: Precipitable water vapour estimation for the dual frequency receivers**

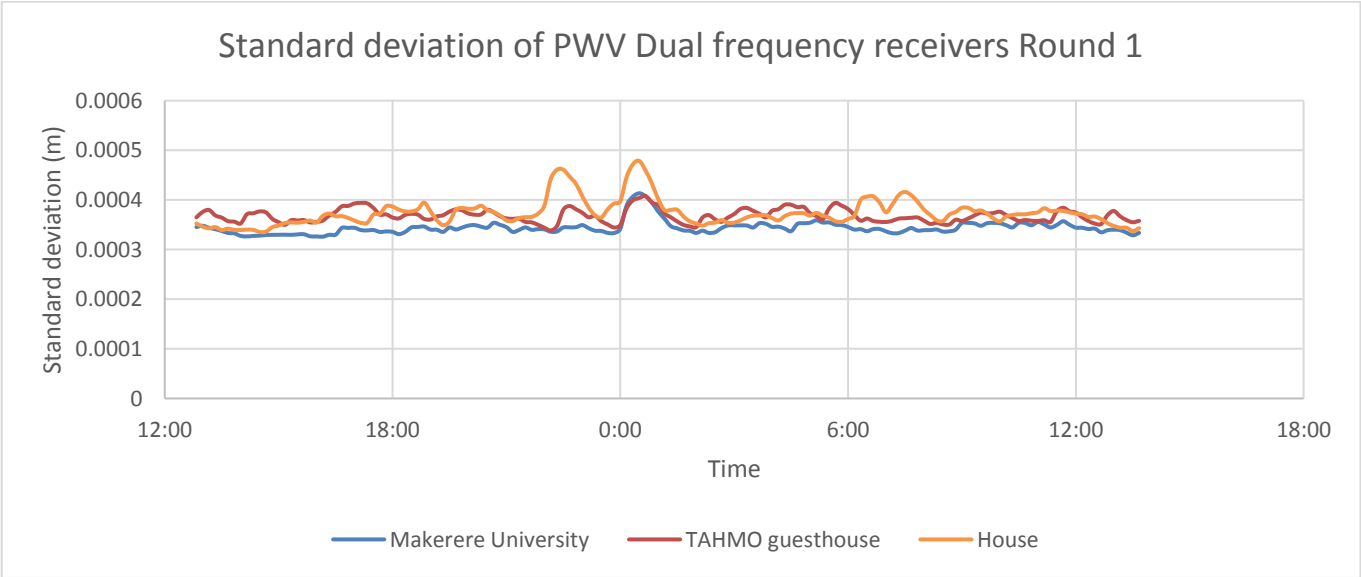


**Figure 6: Standard deviations of the PWV of the dual frequency receivers**

*Single frequency receivers*

In the figures 7 to 10, the PWV estimations are shown for all the working single frequency GPS receivers of round 1. One can immediately notice that there is a lot of variations between the four receivers which was not expected since the receivers were located close to each other. If we take a closer look, sort of a trend could be spotted between the four receivers. They all seem to start with a low PWV around 18.00 and then increases until 06.00 after which it decreases again. Another notable thing is that the estimated PWV of the Hotel location, in figure 8, shows a negative PWV estimation. From now on we assume that this means a PWV estimation of 0 m.

The standard deviations of the single frequency receivers are a lot higher than the standard deviations of the dual frequency receivers. To show this clearer than in figures 7 to 10, the standard deviations of the PWV of the single frequency receivers is plotted in figure 11. The standard deviations are now ranging between 0.3 cm and 0.9 cm which gives an error of about 15% to 50%. One can see through the time that the standard deviation is decreasing with the time. This especially is true for the single frequency receiver at the Hotel location. The measurement line taken here was also longest and as Mariska Koning reported in her part of this research, it is important to measure as long as possible to decrease the standard deviation (Koning, 2016). Also the multipath effect was least on this single frequency receiver since it was placed on a high building with not many other objects in the surrounding.

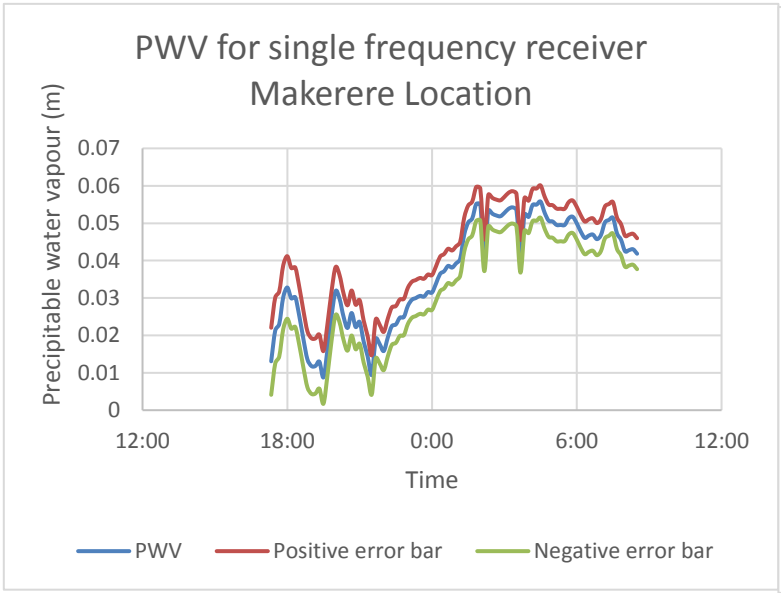


Figure 7: Precipitable water vapour estimation with error bars for the single frequency receiver at the Makerere University location.

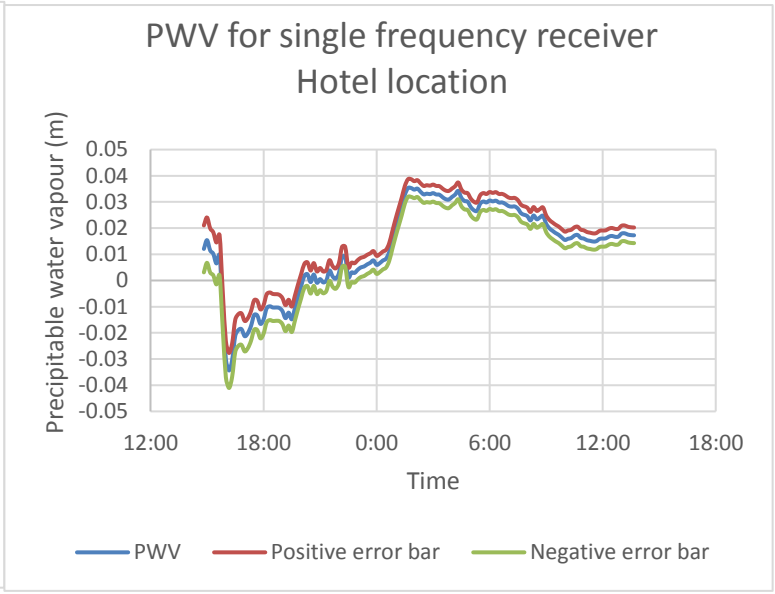


Figure 8: Precipitable water vapour estimation with error bars for the single frequency receiver at the Hotel location.

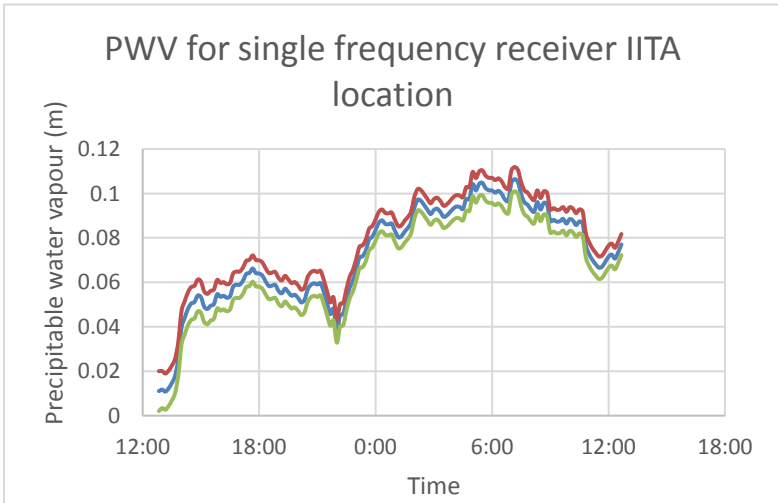


Figure 9: Precipitable water vapour estimation with error bars for the single frequency receiver at the IITA location.

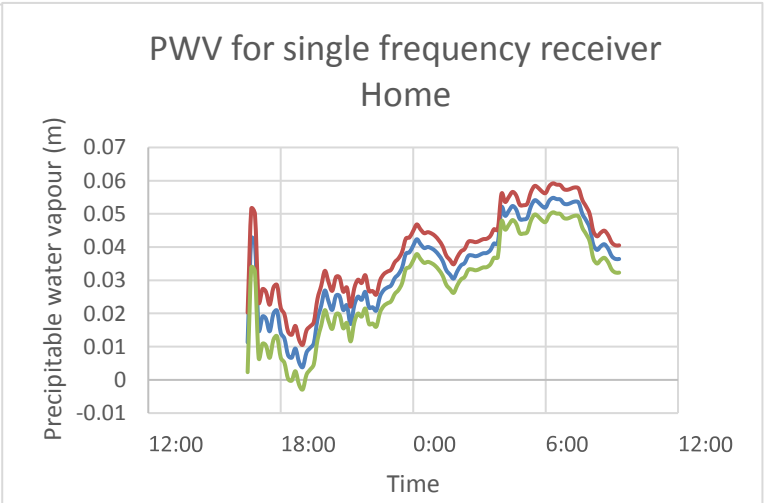


Figure 10: Precipitable water vapour estimation with error bars for the single frequency receiver at the Home location

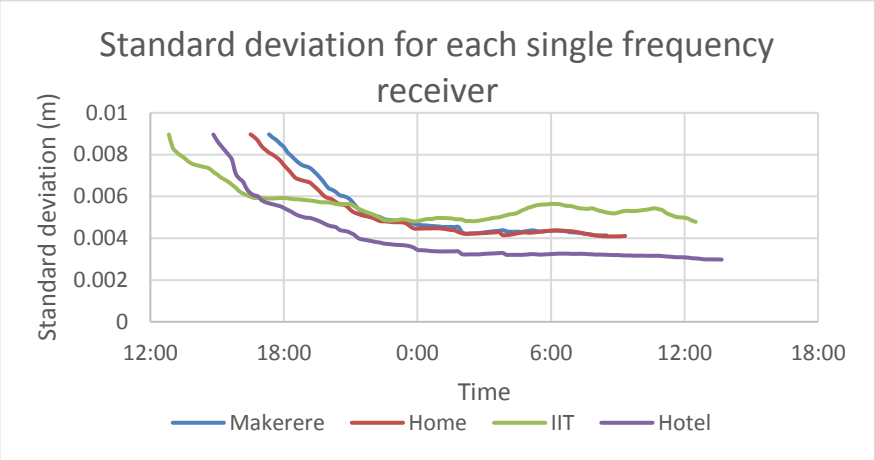


Figure 11: Standard deviations of the single frequency receivers.

## 5.2 Measurement round 3

During measurement round 3 three dual frequency receivers were placed around Uganda together with 6 single frequency receivers in between the dual frequency receivers. Table 2 gives an overview of the performance of all those receivers.

Table 2: Overview of devices and their performance during measurement round 3.

| Receiver | Location | Logging time (UTC+3) | Remarks |
|---|---|---|---|
| Dual 1 | Makerere University | 23 Oct 03:00-<br>28 Oct 20:00 | - |
| Dual 2 | Ndejje Secondary School | 22 Oct 03:00-<br>27 Oct 11:30 | - |
| Dual 3 | Wanyange Girls Secondary School | 22 Oct 03:00-<br>27 Oct 19:15 | - |
| Single 1 | World Ahead Senior Secondary School | 25 Oct 12:25-<br>26 Oct 14:55 | - |
| Single 2 | Makerere high school | 25 Oct 11:35-<br>26 Oct 15:55 | - |
| Single 3 | Homeland College | 25 Oct 15:50-<br>27 Oct 06:55 | - |
| Single 4 | Colline Hotel | 25 Oct 17:20-<br>26 Oct 00:50 | Multipath error, many buildings in the surrounding and turned off quickly |
| Single 5 | African Village Hotel | 25 Oct 18:30-<br>26 Oct 03:35 | - |
| Single 6 | Makerere University | 25 Oct 20:45-<br>26 Oct 13:45 | - |

### 5.2.1 PWV estimations with their standard deviations

With the same method used as during the first measuring round, the precipitable water vapour estimations for the dual and single frequency receivers are calculated using equation 8. The PWV estimation for round 3 for the dual frequency receivers is shown in figure 12. The standard deviations calculated using equation13. for the dual frequency receivers are shown in figure 13. For the single frequency receivers the PWV estimation is plotted with a positive and negative error bar based on the calculated standard deviation. These results are shown in figures 14 to 19.

*Dual frequency receivers*

In figure 12 the precipitable water vapour estimation for the three dual frequency receivers is shown. The graphs show a slightly lower precipitable water vapour estimation than during round 1. The PWV during this round is around 1.8 cm. One things that the notable is, that the three graphs show slightly the same pattern, they all peak around 12.00 on the 26th of October and at the end, around 01.00. When we have a look at the standard deviations of the PWV of the dual frequency receivers, one can see that the values are similar to the standard deviations measured in round 1. The standard deviation is around 0.35 mm and does not improve more. This means there is an error of about 1.8%. The standard deviation of the Makerere dual frequency receiver is lowest. This might have to do with the fact that this receiver was measuring for the longest period of time.

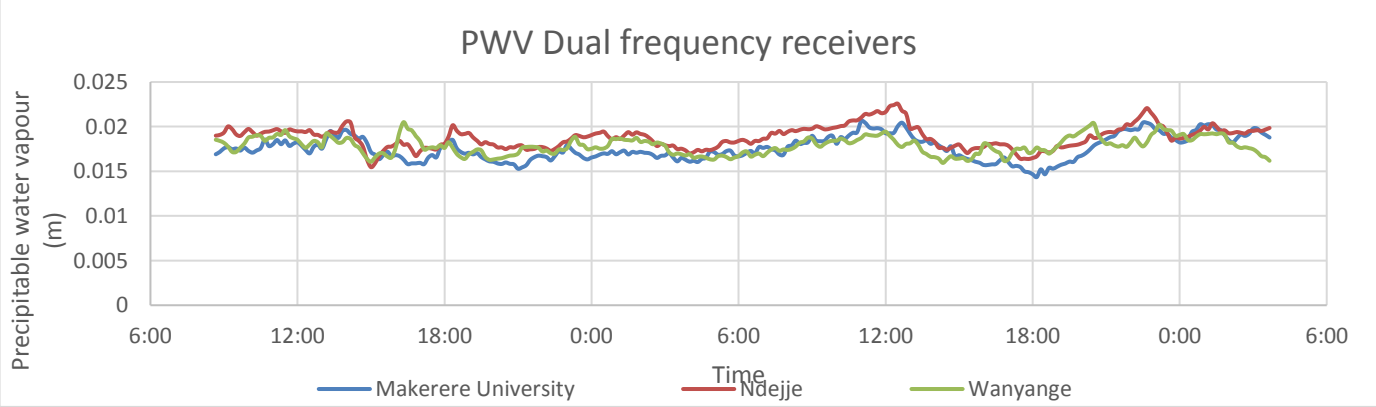


**Figure 12: Precipitable water vapour estimation for the dual frequency receivers. This measurement round started on the 25th of October and ended on the 27th of October.**

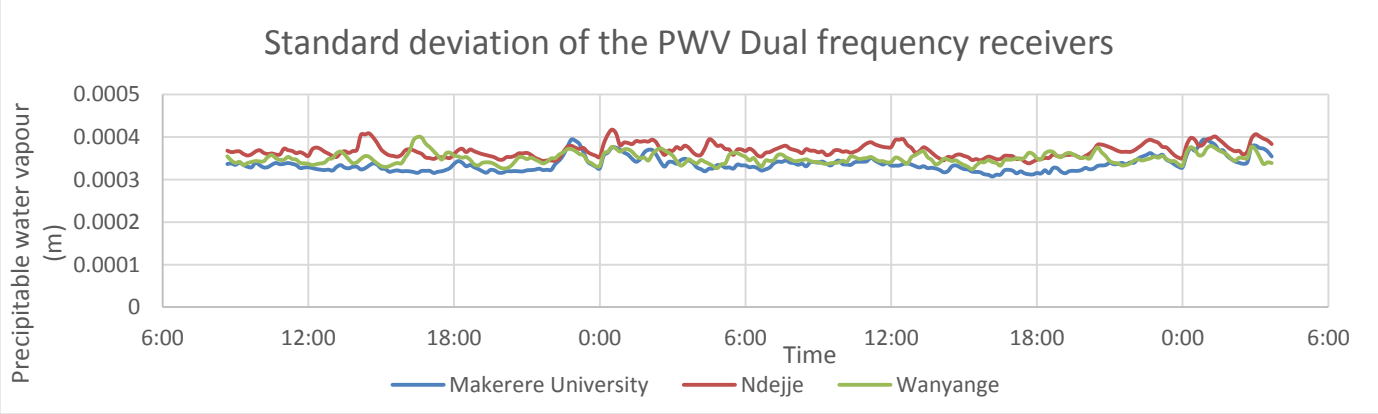


**Figure 13: Standard deviations of the PWV of the dual frequency receivers. This measurement round started on the 25th of October and ended on the 27th of October.**

*Single frequency receivers*

In figures 14 to 19 the PWV estimations of the single frequency receivers with a positive and negative error bar are shown. There is a high variation between all the receivers. The precipitable water vapour is ranging between 0 cm to 0.9 cm. Again one can notice that there are sometimes negative values of the precipitable vapour occurring. We assume this to be 0 cm.

Remarkable is the difference in error bar thickness between the six single frequency receivers. It is clear that some of those have a lower standard deviation than others such as the one at the World Ahead school and Homeland school. The receivers which were located at the African Village hotel and the Coline Hotel have the largest standard deviation. This has most probably to do with their locations. These receivers were both located on the top of an hotel. On those rooftops there were water tanks and TV satellites positioned as well. The objects have most probably disturbed the signal. This is a case of multipath. When we have a better look at the error bars, one can notice that they decrease with the time which we also expect. A better view of this is given in figure 20 in which all the standard deviations are plotted together in one chart. The standard deviations are ranging from 3 mm to 9 mm. This means there is an error of between 7.5% to 45% which is not very sufficient for this research.

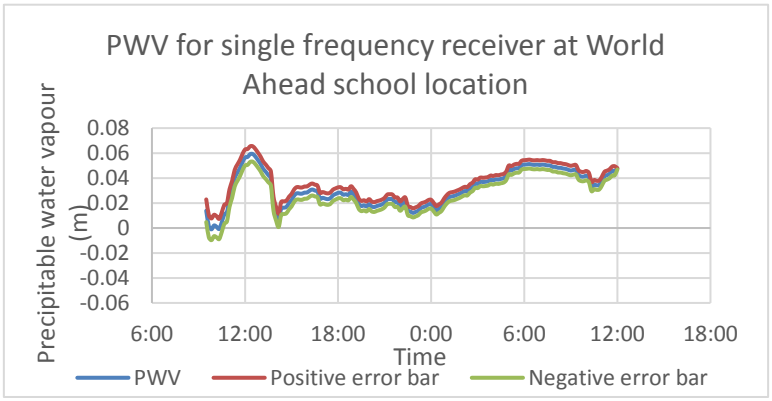


Figure 14: Precipitable water vapour estimation with error bars for the single frequency receiver at the World Ahead school location.

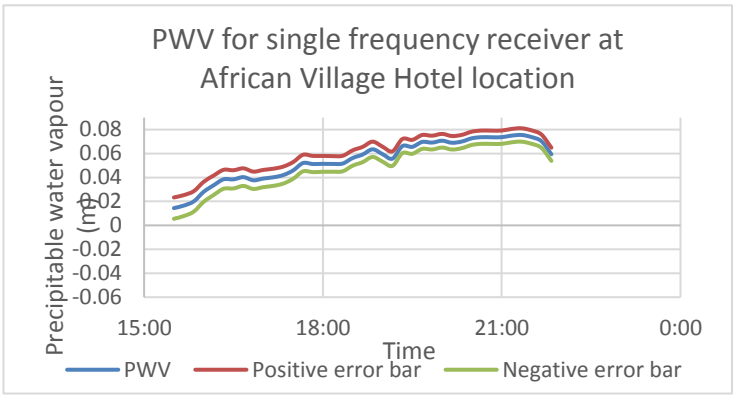


Figure 15: Precipitable water vapour estimation with error bars for the single frequency receiver at the African Village Hotel location.

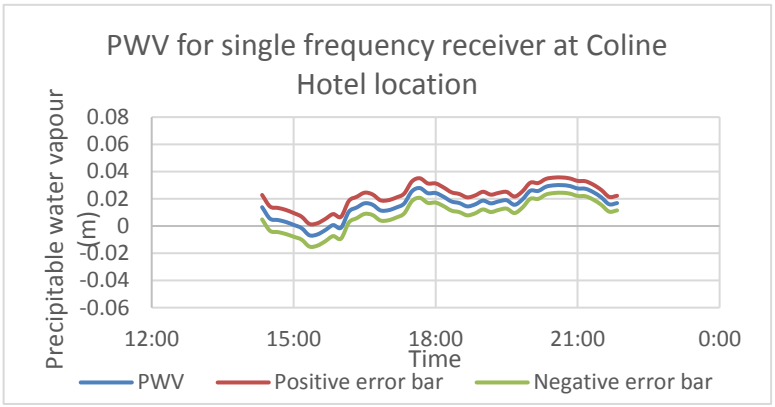


Figure 12: Precipitable water vapour estimation with error bars for the single frequency receiver at the Coline Hotel location.

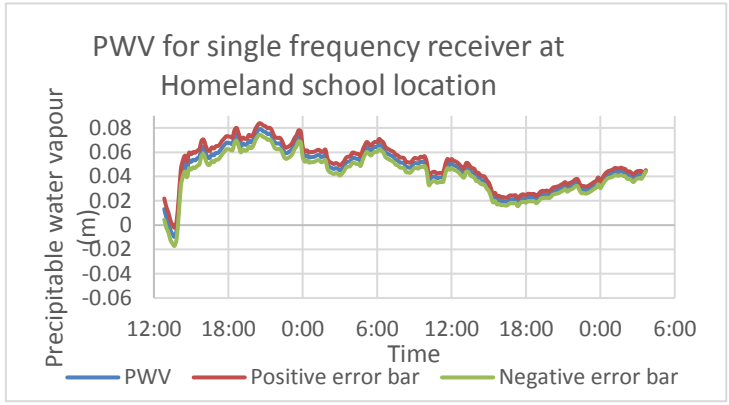


Figure 12: Precipitable water vapour estimation with error bars for the single frequency receiver at the Homeland school location.

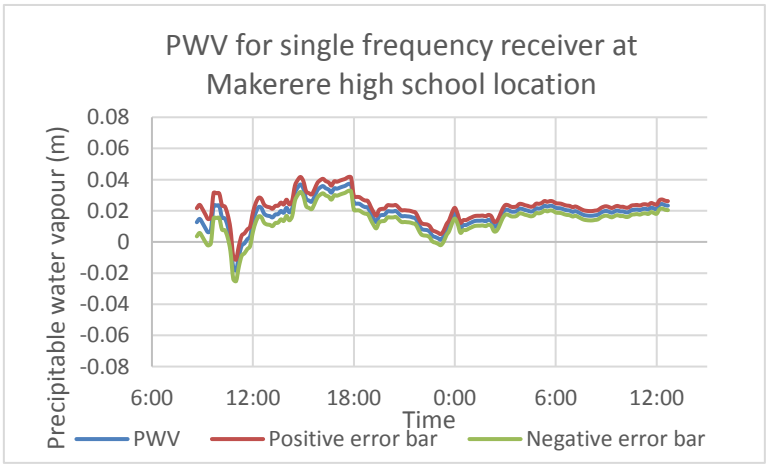


Figure 12:Precipitable water vapour estimation with error bars for the single frequency receiver at the Makerere high school location.

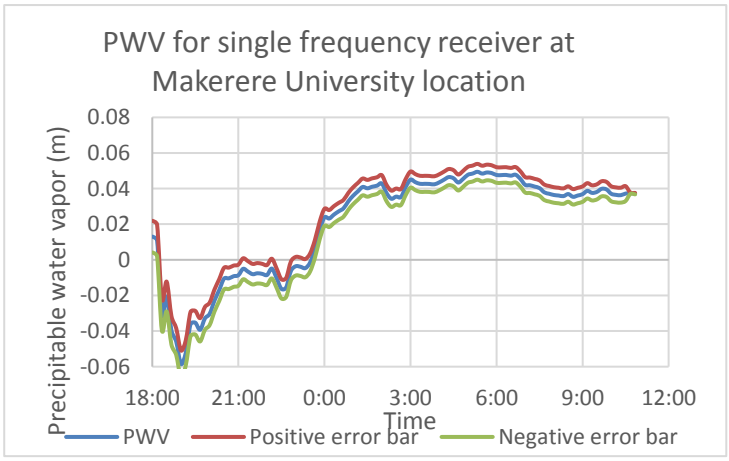


Figure 12: Precipitable water vapour estimation with error bars for the single frequency receiver at the Makerere University location.

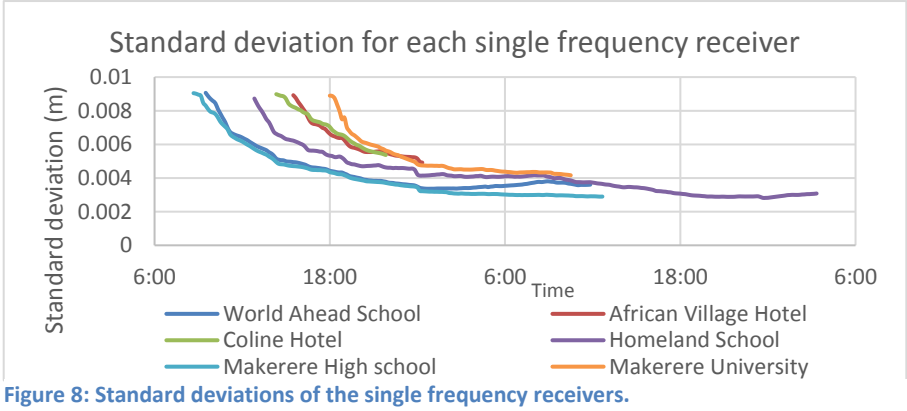


Figure 8: Standard deviations of the single frequency receivers.

## 5.3 Comparison between dual frequency and single frequency receivers.

During both measuring rounds, a dual and single frequency receiver were set up at the same location, namely at the Makerere University. This was done to compare the results of both. For round 1 the precipitable water estimations for the dual and single frequency receiver are plotted together in figure 21. It is clearly shown that there is no correlation at all which is abnormal because the weather conditions and multipath conditions must have been at least very similar. The only thing we can say about these graphs is that they are both showing values for the PWV of around 0.02 m.

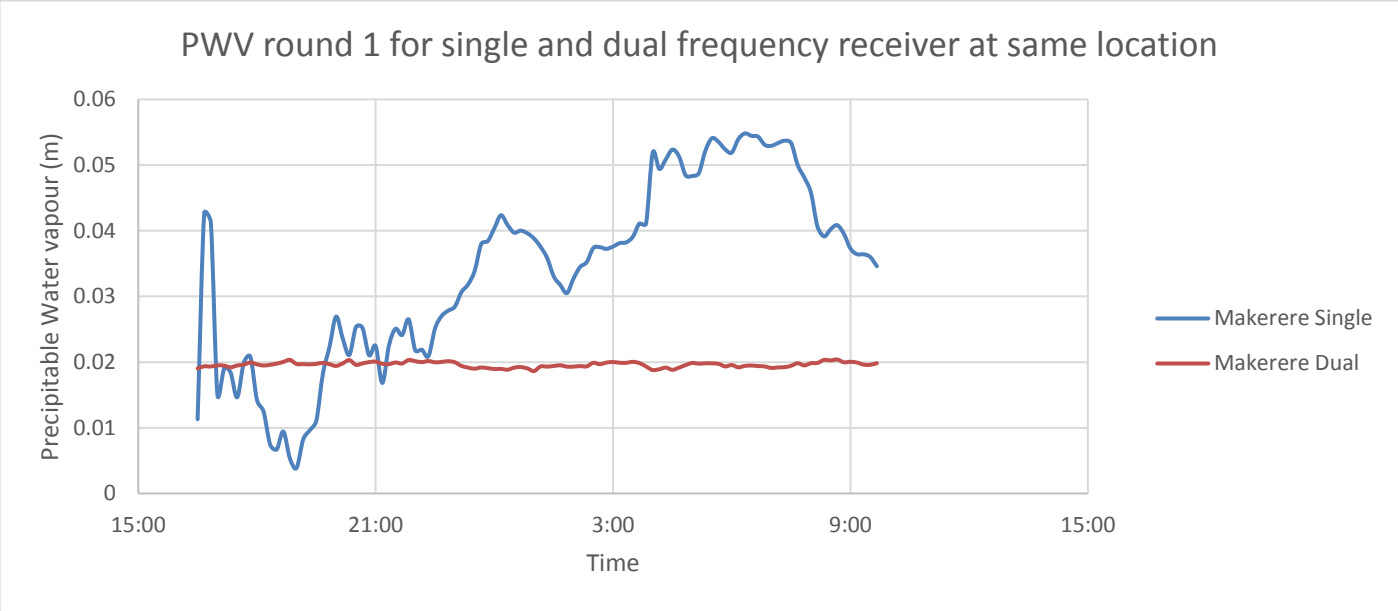


**Figure 21: Precipitable water vapour estimation for a single and dual frequency receiver at the same location, Makerere University. the measurements for this measurement round were taken on the 27th and 28th of September.**

The PWV estimations for the single and dual frequency receiver at the Makerere university are plotted together in figure 22. Again one can notice that there is no correlation between the two graphs. Also as said for round 1, the value for the PWV is always around 0.02 m. Another thing which can be noticed is that both PWV estimations for the single frequency receivers start with a dip and then increase again.

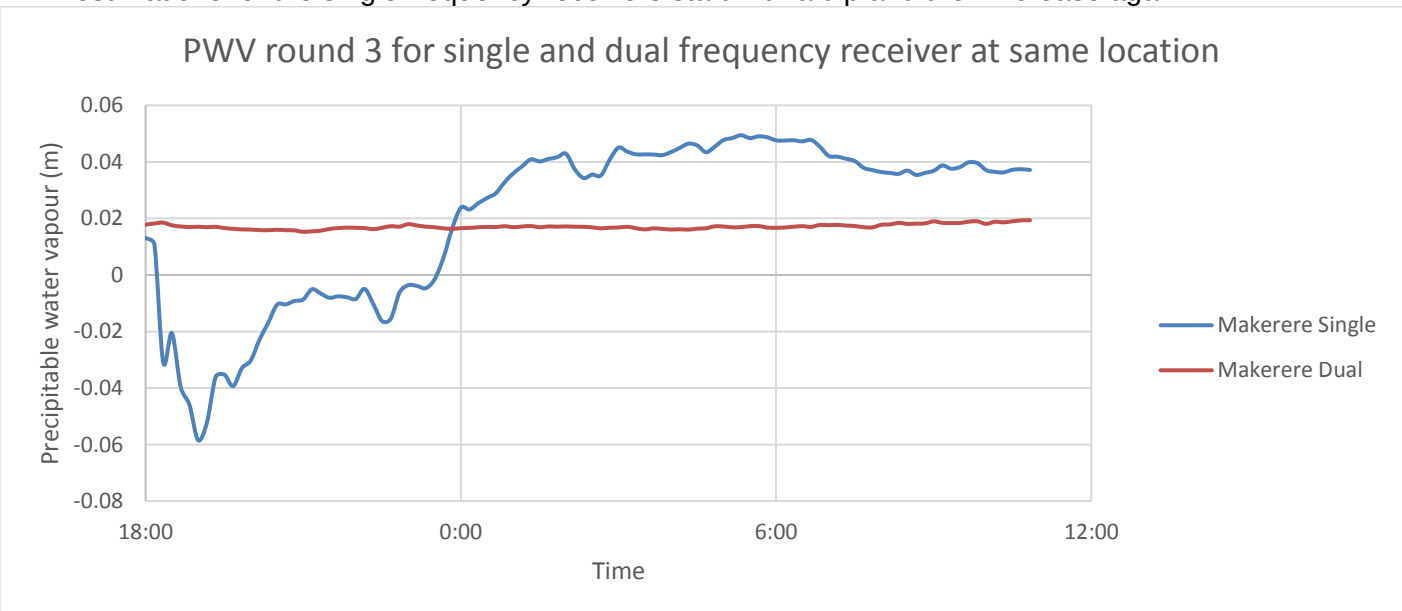


**Figure 22: Precipitable water vapour estimation for a single and dual frequency receiver at the same location, Makerere University. the measurements for this measurement round were taken on the 25th and 26th of October.**

# 6 Conclusion

As can be read in the report of Mariska Koning (Koning, 2016), the u-blox M8T single frequency receivers were not precise nor accurate. This followed in precipitable water vapour estimations which were not sufficient for the purpose they want to be used for.

In the results & discussion chapter, it was shown that the PWV estimations were for both measuring rounds not very precise. In all the estimations for the PWV of single frequency receivers there was a large scatter of values around the 0.02 m. About the accuracy we cannot say anything so far since we do not know the exact value for the precipitable water vapour. Though we can say that the values of the single frequency receivers are around the 'right' value if you consider the 0.02 m of the dual frequency PWV estimations the right one.

Another point to mention, is the fact that receivers located at a location where a lot of multipath existed, have very high standard deviations. This was clearly shown with the results of measurement round 3. If the receivers would be placed in Uganda, it is thus or great importance that they will have a clear view to the sky and do not experience a lot of multipath effects.

The Trimble dual frequency receivers got precise results with low standard deviations in both measurement rounds. A precipitable water vapour value of around 0.02 m is a reasonable value according to NASA/JPL (NASA/JPL, 2016) and (Tsidu, Blumenstock, & Hase, 2015). With these result it can be concluded that the Saastamoinen model fits well, though it should be taken into consideration that a real validation is not done yet.

The interpolation method, inverse distance interpolation, works well. This can be concluded from the fact that the PWV estimations at the Makerere university in round 3 are similar to the PWV estimations of the Ndejje school and the Wanyange school. At the Ndejje and Wanyange school a TAHMO weather station provided the weather data for this PWV estimation. At the Makerere university no weather data was available and weather data needed to be interpolated from the Entebbe, Mityana, Ndejje and Wanyange weather station locations.

At the moment the u-blox M8T are not suitable for precipitable water vapour estimation yet. Nevertheless, further research could improve the result. Therefore we recommend further research in the future as can be read in the next chapter.

# 7 Recommendations

One of the main problems faced during this project was the shortage of power supply. Therefore measuring with the u-blox receivers was difficult and measuring more than 24 hours was almost impossible. To reduce the standard deviation and the variations in the measurements, it is highly recommend to take more measurements for a longer period of time. As Mariska Koning stated, the standard deviation of the ZTD estimations will decrease when the measuring device has a longer period of time to measure. This was also seen at the dual frequency receivers. The dual frequency receivers has a very high precision while the single frequency receivers has not.

Another thing to mention, is the lack of weather data. Since this research was meant to give precise estimations for the precipitable water vapour it is of great importance that the weather measurements are precise as well. In this research we used interpolation techniques to receive weather data at all locations of the GPS station locations. Though this is not ideal and therefore I would like to recommend to have weather stations at least at every location of the dual frequency receivers.

In this research the Saastamoinen model was used to derive the precipitable water vapour estimations. This model fits well, but further research should be done in order to be sure that the right model is the Saastamoinen model. Due to time limitations and the lack of radiosonde data the obtained PWV estimations could not be validated as well. Future research should find out whether or not the obtained values are the real and accurate values. Another method of validation could be the comparison between satellite image and the PWV estimations. In this way at least clouds could be observed and related to the obtained PWV values. MERIS data seems the most suitable for this (Lindenbergh, Keshin, Marel, & Hanssen, 2008).

Last but not least, I want to mention that setting up dual frequency receivers instead of single frequency receivers everywhere is the ideal solution. At the moment this is too expensive, but u-blox is working on an affordable dual frequency GPS receiver which might be a solution for this project. The dual frequency receivers are most probably always more precise and accurate than the single frequency receivers, since you are not working with interpolation methods which are decreasing the measurements precision.

# Bibliography


C. Rocken, J. B. (2000). GPS Networks for Atmospheric Sensing. ION National Technical Meeting, Anaheim, CA.

Clark, D. (2012, 09 19). How will climate change affect food production? *The Guardian*.

D. E. Wolfe, S. I. (1999). Developing an Operational, Surface-Based, GPS, Water Vapor Observing System for NOAA: Network Design and Results. In *Journal of atmospheric and oceanic technology.* Ninth ARM Science Team Meeting Proceedings, San Antonio, Texas.

Deng, Z. (2009). *Retrieving tropospheric delays from GPS networks densified with single frequency receivers.* GEOPHYSICAL RESEARCH LETTERS.

E. R. Westwater, Y. H. (1998). Remote sensing of total precipitable water vapor by microwave radiometers and GPS during the 1997 Water Vapor Intensive Operating Period. Seatle, WA.

Enge, P., & Misra, P. (2001). *Global Positioning System* (1 ed.). Ganga-Jamuna Press.

Enge, P., & Misra, P. (2006). *Global Positioning System* (2 ed.). Ganga-Jamuna Press.

ESA. (2016, September 30). *Our activities Launching Galileo*. Retrieved from ESA: http://www.esa.int/Our_Activities/Navigation/Galileo/Launching_Galileo/And_yet_it_moves_14_Galileo_satellites_now_in_orbit

Gabor, M. (1997, May 5). *Remote Sensing of Water Vapor from GPS Receivers*. Retrieved May 16, 2016, from http://www.csr.utexas.edu/texas_pwv/midterm/gabor/gabor.html#anchor561367

Haan, S. d. (2008). *Meteorological applications of a surface network of Global Positioning System receivers.*

Information World Weather & Climate. (2016). *Average Monthly Weather in Gulu, Uganda*. Retrieved 09 25, 2016, from https://weather-and-climate.com/average-monthly-Rainfall-Temperature-Sunshine,Gulu,Uganda

J. Braun, C. R. (1999). Development of a Water Vapor Tomography System Using Low Cost L1 GPS Receivers. In *Journal of atmospheric and oceanic technology.* Ninth ARM Science Team Meeting Proceedings, San Antonio, Texas.

J.M.Rüeger. (2002). Refractive Index Formulae for Radio Waves. *Integration of Techniques and Corrections to Achieve Accurate Engineering* (pp. 1-13). Washington: International Congress.

K. Yedukondalu, A. S. (2011). Estimation and Mitigation of GPS Multipath Interference Using Adaptive Filtering. *Progress in Electromagnetics Research M*(21), 133-148.

Koning, A. (2016). *Precipitable water vapour estimation using GPS in Uganda: A study on obtaining the Zenith Wet Delay.* Delft, The Netherlands.

Lambert Wanninger, Institut für Erdmessung, Universität Hannover. (1993, July). Effects of the equatorial ionosphere on GPS. *GPS world*, 48-54.

Lindenbergh, R., Keshin, M., Marel, H. v., & Hanssen, R. (2008). COMBINING WATER VAPOR DATA FROM GPS AND MERIS. In T. Reuters, *International Journal of Remote Sensing Vol. 29* (pp. 2393-2409). : 2016 Journal Citation Reports.

M. Bender, G. D. (2009). Estimates of the information provided by GPS slant data observed in Germany regarding tomographic applications. In *JOURNAL OF GEOPHYSICAL RESEARCH.*

M. Bevis, S. B. (1994). *GPS Meteorology: Mapping Zenith Wet Delays onto Precipitable Water.* Colorado: American Meteorological Society.

M.C. Eckl, R. S. (2001). Accuracy of GPS-derived relative positions as a function of interstation distance and observing-session duration. In *Journal of Geodesy* (pp. 633-640). Springer-Verlag.

NASA/JPL. (2016, 12 10). *Global Total Precipitable Water Vapor for May 2009*. Retrieved from Jet Propulsion Laboratory, California Institute of Technology: http://www.jpl.nasa.gov/spaceimages/details.php?id=PIA12096

Nicholas Zinas. (2016, October 04). *Satellite and receiver clock Errors*. Retrieved from Tekmon Geomatics: http://www.tekmon.eu/1-3-2-satellite-and-receiver-clock-errors/

S. Amir, T. M. (2011). GPS Meteorology Activities in the Malaysian Peninsula. In *Journal of Atmospheric and Solar-Terrestrial Physics* (pp. 2410-2422). Universiti Teknologi Malaysia (UTM), 81310 Skudai, Johor Malaysia.

Shrestha, S. (2003). *Investigations into the Estimation of Tropospheric Delay and Wet Refractivity Using GPS Measurements.* Calgary, Canada.
TAHMO. (n.d.). *TAHMO*. Retrieved 04 31, 2016, from www.tahmo.org
Thomas F. Stocker, Q. D.-K. (2015). *Technical Summary.* IPCC. Cambridge, United Kingdom and New York, United States: Cambridge University Press.
Tsidu, G. M., Blumenstock, T., & Hase, F. (2015). *Observations of precipitable water vapour over complex topography of Ethiopia from ground-based GPS, FTIR, radiosonde and ERA-Interim reanalysis.* Atmospheric Measurement Techniques.
UNMA. (2016, September 30). *Seasonal Forecasts*. Retrieved from Uganda National Meteorological Authority: https://www.unma.go.ug/index.php/climate/seasonal-forecasts
V.B.Mendes, & R.B.Langley. (1999). Tropospheric Zenith Delay Prediction Accuracy for Airborne GPS High-Precision Positioning. Fredericton, Canada.
Wackernagel, H. (2003). *Multivariate Geostatistics 3rd edition.* Berlin, Germany: Springer.
Yoshinori Shoji, H. Y. (2014). Estimation of Local-scale Precipitable Water Vapor Distribution Around Each GNSS Station Using Slant Path Delay. In *SOLA* (pp. 29-33).
Yuan, Y. K.-S. (2014). Real-time retrieval of precipitable water vapor from GPS precise point positionin. *Journal of geophysical research: Atmospheres*.

# Appendix

## *Read out Trimble 5700 with DataTransfer programme*

1. Turn off the data logging by pressing the data button for 3 seconds.
2. Disconnect the power supply from the cable and connect the middle output with the VGA to USB and put in computer
3. Start DataTransfer software and press devices.
4. Press new and select the GPS Receiver (R/SPS/ 5000 series).
5. For the port, select the COM6 port.
6. In the COM6 port menu every setting is left untouched.
7. Click in the window part of 'Files to Receive' on Add
8. Select all the files you want to transfer and put a directory to transfer to.
9. Click transfer all
10. When the transfer has taken place, you have both the .T01 and .DAT files, that still need to be converted. Use the programme 'Convert to RINEX' to do this.

## *Convert T01 data to RINEX*

Use the programme 'Convert to RINEX'

1. Click on the dropdown menu 'file' and press 'open'.
2. Select the files you want to convert.
3. Again, click on the dropdown menu 'file' and press 'convert files'.
4. The converted files can be found in the same folder as the original files.